New Journal of Physics
The open access journal at the forefront of physics

Deutsche Physikalische Gesellschaft DPG
IOP Institute of Physics

Published in partnership with: Deutsche Physikalische Gesellschaft and the Institute of Physics

OPEN ACCESS

RECEIVED
12 April 2015

REVISED
16 July 2015

ACCEPTED FOR PUBLICATION
17 July 2015

PUBLISHED
17 August 2015

PAPER

Post-selected von Neumann measurement with Hermite–Gaussian and Laguerre–Gaussian pointer states

Yusuf Turek[1,2], **Hirokazu Kobayashi**[3], **Tomotada Akutsu**[4,5], **Chang-Pu Sun**[6] **and Yutaka Shikano**[1,7,8]

[1] Research Center of Integrative Molecular Systems (CIMoS), Institute for Molecular Science, National Institutes of Natural Sciences, Okazaki, Aichi 444-8585, Japan
[2] State Key Laboratory of Theoretical Physics, Institute of Theoretical Physics, Chinese Academy of Sciences, and University of the Chinese Academy of Sciences, Beijing 100190, People's Republic of China
[3] Department of Electronic and Photonic System Engineering, Kochi University of Technology, Tosayamada-cho, Kochi 782–0003, Japan
[4] National Astronomical Observatory of Japan, Mitaka, Tokyo 181-8588, Japan
[5] Department of Astronomical Science, The Graduate University for Advanced Studies (SOKENDAI), Mitaka, Tokyo 181-8588, Japan
[6] Beijing Computational Science Research Center, Beijing 100084, People's Republic of China
[7] Institute for Quantum Studies, Chapman University, Orange, CA 92866, USA
[8] Materials and Structures Laboratory, Tokyo Institute of Technology, Yokohama 226-8503, Japan

E-mail: yusufu@itp.ac.cn, kobayashi.hirokazu@kochi-tech.ac.jp, cpsun@csrc.ac.cn **and** yshikano@ims.ac.jp

Keywords: von Neumann interaction, quantum measurement, weak measurement, higher-order Gaussian mode, signal-to-noise ratio, weak-value amplification

Abstract

Through the von Neumann interaction followed by post-selection, we can extract not only the eigenvalue of an observable of the measured system but also the weak value. In this post-selected von Neumann measurement, the initial pointer state of the measuring device is assumed to be a fundamental Gaussian wave function. By considering the optical implementation of the post-selected von Neumann measurement, higher-order Gaussian modes can be used. In this paper, we consider the Hermite–Gaussian (HG) and Laguerre–Gaussian (LG) modes as pointer states and calculate the average shift of the pointer states of the post-selected von Neumann measurement by assuming the system observable $\hat{A}$ with $\hat{A}^2 = \hat{I}$ and $\hat{A}^2 = \hat{A}$ for an arbitrary interaction strength, where $\hat{I}$ represents the identity operator. Our results show that the HG and LG pointer states for a given coupling direction have advantages and disadvantages over the fundamental Gaussian mode in improving the signal-to-noise ratio. We expect that our general treatment of the weak values will be helpful for understanding the connection between weak- and strong-measurement regimes and may be used to propose new experimental setups with higher-order Gaussian beams to investigate further the applications of weak measurement in optical systems such as the optical vortex.

1. Introduction

In a quantum measurement, observable information in the measured system can be extracted from the statistical average shift of a pointer. In this process, von Neumann interaction is initially used with the standard model of quantum measurement by mathematically describing the coupling between the measured system and measuring devices [1]. However, such strong measurements are not time symmetric. When considering time-symmetric quantum measurements, post-selection of the measured system is required after the measurement interaction [2]. On summing the post-selections, the statistical average shift of the pointer can be determined in the standard model of quantum measurement. Therefore, throughout the present work, measurements with post-selection are called post-selected von Neumann quantum measurements. A particular case of post-selected von Neumann quantum measurements with sufficiently weak coupling between the measuring device and measured system is called the weak measurement, as proposed by Aharonov *et al* [3]. This statistical average shift of the pointer is characterized by the weak value of the observable in the measured system [4].

A significant feature of the weak measurements is that the weak value of the measured quantity can lie outside the usual range of eigenvalues of an observable applicable for a standard quantum measurement [3]. This feature is usually referred to as the amplification effect for weak signals and is different from conventional quantum measurement, in which a coherent superposition of quantum states is collapsed [1]. A large weak value can amplify small unknown parameters for detecting various properties such as beam deflection [5–10], frequency shifts [11], phase shifts [12], angular shifts [13, 14], velocity shifts [15], and even temperature shifts [16]. However, the advantages of the weak-value amplification are purely technical [17–25]. This is based on the single parameter estimation theory. In general, the weak value is a complex number. Thus, weak measurements are ideal for examining the fundamentals of quantum physics such as quantum paradoxes (Hardy's paradox [26–29] and the three-box paradox [30]), quantum correlation and quantum dynamics [31–39], and quantum-state tomography [40–45], as well as the violation of the generalized Leggett–Garg inequalities [46–51] and the violation of the initial Heisenberg measurement–disturbance relationship [52, 53].

Thus far, most studies on weak measurement use the zero-mean Gaussian state as an initial pointer state and expand the unitary operator of evolution up to the first order because, in the weak measurement scheme, the coupling between the measured system and measuring device is very weak. However, when considering the connection between weak and strong measurements, amplification limit, and measurement back-action of the weak measurement scheme, the full-order effects of unitary evolution due to the von Neumann interaction between the measured system and measuring device are required. The measurements of arbitrary coupling strength beyond the first-order interaction have been previously discussed by Aharonov and Botero [54]. Di Lorenzo and Egues [55] investigated von Neumann-type measurement to clarify detector dynamics in the weak-measurement process. Wu and Li [56] proposed a general formulation of weak measurement that includes second-order effects of the unitary evolution due to the von Neumann interaction between the system and detector, and they theoretically demonstrated on the basis of the second-order calculation that the back-action effect is important in the weak-value amplification. Recently, several studies [57–59] analytically showed that an upper bound of the weak-value amplification exists in the post-selected von Neumann measurement by assuming that the probe-state wave function is Gaussian and that the observable $\hat{A}$ satisfies $\hat{A}^2 = \hat{I}$, where $\hat{I}$ is the identity operator. On the other hand, there is no upper bound on the weak-value amplification on the optimal probe-state wave function [60–62] while it is so difficult to implement this wave function [63].

In optical experiments, we encounter higher-order Gaussian beams such as Hermite–Gaussian (HG) and Laguerre–Gaussian (LG) beams, which are higher-order solutions of the paraxial wave equation with rectangular and cylindrical symmetry about their axes of propagation, respectively. Both HG and LG beams are widely used in the theory of lasers and resonators [64, 65]. In fact, the zero-mean Gaussian beam is a special case of HG and LG beams. The weak measurement with the higher-order Gaussian-beam pointer state has been discussed in [66–70]. In particular, de Lima Bernardo *et al* [70] presented a simplified algebraic description of the weak measurements with HG and LG pointer states. In [70], the unitary evolution operator is considered only up to the first order, raising an intriguing question as to whether the higher-order Gaussian beams are more advantageous in quantum measurement compared to the fundamental Gaussian beam.

In the present study, we determine the post-selected von Neumann quantum measurement for an arbitrary coupling strength with HG- and LG-mode pointer states under the assumption that the system observable $\hat{A}$ satisfies $\hat{A}^2 = \hat{I}$ and $\hat{A}^2 = \hat{A}$ (projection operator). To clarify the practical advantages of higher-order Gaussian beams, we investigate the signal-to-noise ratio (SNR) while considering the post-selection probability, which is defined by

$$\mathrm{SNR}_W = \frac{\sqrt{NP_s}\,\left|\langle W\rangle_{fi}\right|}{\sqrt{\left\langle W^2\right\rangle_f - \langle W\rangle_f^2}}, \quad \hat{W} = \hat{X},\ \hat{Y}. \tag{1}$$

Here, $\langle\,.\,\rangle_f$ denotes the expectation value of the measuring system operator under the final state of the pointer, and $\hat{X} = \int x\ |x\rangle\langle x|\ \mathrm{d}x$ (x is the coupling direction of the von Neumann measurement) and $\hat{Y} = \int y\ |y\rangle\langle y|\ \mathrm{d}y$ (y is the orthogonal coupling direction). Here, P_s is the probability that the post-selected state is included in the pre-selection state, and N is the number of measurement time. To verify our general formulas, two special limits are considered. If the zero-mean Gaussian pointer is used as the initial state, our general expectation values are found to reduce to the results given in [56, 59]. On the other hand, if the evaluation is considered only up to the first order, our general expectation values reproduce all results given in [70].

The remainder of this paper is organized as follows. In section 2, we present the model setup for the post-selected von Neumann measurement. In sections 3 and 4, we first present the expressions of HG- and LG-mode pointer states in the Fock-state representation in accordance with de Lima Bernardo *et al* [70]. We then present general forms of the expectation values and discuss the SNRs with HG- and LG-mode pointer states for the system operator $\hat{A}$ with $\hat{A}^2 = \hat{I}$ and $\hat{A}^2 = \hat{A}$, which were used in several optical implementation on the weak

measurement [5–16, 30, 47, 52, 53, 69]. In section 5, to check the validity of our general results, we consider some special initial pointer states and approximated treatments used in previous works and show that our general formulas can reproduce all the related results reported in those previous works [56, 59, 70]. We present the conclusions and remarks of our study in the final section 6. Throughout this paper, we use $\hbar = 1$ units.

2. Model setup

For the post-selected von Neumann measurement, the coupling interaction between the system and detector is considered with the standard von Neumann Hamiltonian:

$$H = g\delta\left(t - t_0\right)\hat{A} \otimes \hat{P}_x, \tag{2}$$

where g is a coupling constant and $\hat{P}_x$ is the conjugate momentum operator for the position operator $\hat{X}$ of the measurement device; i.e. $[\hat{X}, \hat{P}_x] = \mathrm{i}\hat{I}$. We have taken the interaction to be impulsive at time $t = t_0$ for simplicity. The time-evolution operator for such impulsive interaction is $\mathrm{e}^{-\mathrm{i}g\hat{A}\otimes\hat{P}_x}$.

The post-selected von Neumann measurement is characterized by the pre- and post-selection of the system state. If we prepare an initial state $|\psi_i\rangle$ of the system and pointer state, after some interaction time t_0, we post-select a system state $|\psi_f\rangle$ and obtain information on a physical quantity $\hat{A}$ from the pointer wave function by using the following weak value:

$$\langle A\rangle_w = \frac{\left\langle \psi_f \left| \hat{A} \right| \psi_i \right\rangle}{\left\langle \psi_f \middle| \psi_i \right\rangle}. \tag{3}$$

In general, the weak value is a complex number. It is evident from equation (3), that when the pre-selected state $|\psi_i\rangle$ and the post-selected state $|\psi_f\rangle$ are nearly orthogonal to each other, the absolute value of the weak value can be arbitrarily large, resulting in the weak-value amplification.

From the above definitions, we note that the unitary evolution operator $\mathrm{e}^{-\mathrm{i}g\hat{A}\otimes\hat{P}_x}$ for the operator $\hat{A}$ satisfies the property $\hat{A}^2 = \hat{I}$ as follows:

$$\mathrm{e}^{-\mathrm{i}g\hat{A}\otimes\hat{P}_x} = \frac{1}{2}\left(\hat{I} + \hat{A}\right) \otimes D\left(\frac{s}{2}\right) + \frac{1}{2}\left(\hat{I} - \hat{A}\right) \otimes D\left(-\frac{s}{2}\right). \tag{4}$$

Similarly, for the property $\hat{A}^2 = A$, the evolution operator satisfies

$$\mathrm{e}^{-\mathrm{i}g\hat{A}\otimes\hat{P}_x} = \left(\hat{I} - \hat{A}\right) \otimes \hat{I} + \hat{A} \otimes D\left(\frac{s}{2}\right). \tag{5}$$

Here, we use the position operators $\hat{X}$ and $\hat{Y}$ as well as their corresponding momentum operators $\hat{P}_x$ and $\hat{P}_y$, which can be written in terms of the annihilation (creation) operators $\hat{a}_i$ ($\hat{a}_i^\dagger$) with $i = x, y$ as [71]

$$\hat{X} = \sigma\left(\hat{a}_x^\dagger + \hat{a}_x\right), \tag{6}$$

$$\hat{Y} = \sigma\left(\hat{a}_y^\dagger + \hat{a}_y\right), \tag{7}$$

$$\hat{P}_x = \frac{\mathrm{i}}{2\sigma}\left(\hat{a}_x^\dagger - \hat{a}_x\right), \tag{8}$$

$$\hat{P}_y = \frac{\mathrm{i}}{2\sigma}\left(\hat{a}_y^\dagger - \hat{a}_y\right). \tag{9}$$

Here, σ is the width of the fundamental Gaussian beam. It is worth noting that in these definitions, the propagation direction of the beam is assumed to be fixed [72]. These annihilation (creation) operators satisfy the commutation relations $[\hat{a}_i, \hat{a}_j^\dagger] = \delta_{ij}\hat{I}$ with $i, j = x, y$. The parameter s is defined as $s: \equiv g/\sigma$, and $D(\xi)$ is a displacement operator with complex ξ defined as

$$D(\xi) = \mathrm{e}^{\xi\hat{a}_x^\dagger - \xi^*\hat{a}_x}. \tag{10}$$

Here, the parameter s characterizes the measurement strength. Note that the interaction between the system and pointer is weak (strong) if $s \ll 1$ ($s \gg 1$).

In the following sections, we consider the post-selected von Neumann measurement with HG- and LG-mode pointer states for an arbitrary measurement-strength parameter s for the system operator $\hat{A}$ with $\hat{A}^2 = \hat{I}$ and $\hat{A}^2 = \hat{A}$, respectively. On the choice of the system operator $\hat{A}$, $\hat{A}^2 = \hat{I}$ and $\hat{A}^2 = \hat{A}$ are taken as the qubit operator and the projector, respectively.

3. Post-selected von Neumann measurements with HG-mode pointer states

The general HG modes can be generated from the fundamental Gaussian mode, $|0,0\rangle_{\rm HG}$, and can be defined as [70, 71]

$$|n,\ m\rangle_{\rm HG} = \frac{1}{\sqrt{n!m!}}\left(\hat{a}_x^{\dagger}\right)^n\left(\hat{a}_y^{\dagger}\right)^m|0,0\rangle_{\rm HG}. \tag{11}$$

These modes are complete sets of solutions to the paraxial wave equation in rectangular coordinates. Any arbitrary paraxial wave can be described as a superposition of HG modes with the appropriate weighting and the phase factors. Practically, the higher-order HG modes can be simply generated by inserting cross wires into the laser cavity with the wires aligned with the nodal lines of the desired HG mode [73, 74]. However, a more convenient way for generating higher-order modes is the use of computer-generated holograms or a spatial light modulator (SLM) [75], which allows reprogrammable waveform generation controlled using a computer.

In the present paper, the initial state of the HG-mode pointer is considered to be $|\phi_i\rangle = |n,\ m\rangle_{\rm HG}$. Note that the HG modes can be factored in functions that depend on x and y directions. In our standard von Neumann measurement Hamiltonian (2), only x-direction interaction exists; thus, the y-direction quantum number m is omitted in the HG-mode calculations.

In what follows, we discuss the post-selected von Neumann measurement for the system operator $\hat{A}$ that satisfies the properties $\hat{A}^2 = \hat{I}$ and $\hat{A}^2 = \hat{A}$.

3.1. $\hat{A}^2 = \hat{I}$ case

After the unitary evolution given in equation (4), the system state is post-selected to $|\psi_f\rangle$. Then, we obtain the following normalized final pointer states:

$$\left|\phi_{f_1}\right\rangle = \frac{\lambda}{2}\left[D\left(-\frac{s}{2}\right) + D\left(\frac{s}{2}\right) + \langle A\rangle_w\left(D\left(\frac{s}{2}\right) - D\left(-\frac{s}{2}\right)\right)\right]|n\rangle_{\rm HG}, \tag{12}$$

where the normalization coefficient is given by

$$\lambda = \left[1 + \frac{1}{2}\left(1 - \left|\langle A\rangle_w\right|^2\right)\left(\mathrm{e}^{-\frac{s^2}{2}}L_n\left(s^2\right) - 1\right)\right]^{-\frac{1}{2}}. \tag{13}$$

Here, the Laguerre polynomials are defined as

$$L_n(x) = \sum_{\epsilon=0}^{n}\binom{n}{\epsilon}\frac{(-1)^{\epsilon}}{\epsilon!}x^{\epsilon}. \tag{14}$$

The explicit expression of equation (12) can be obtained using the displaced Fock states defined as [76, 77]

$$D(\xi)|n\rangle_{\rm HG} = \mathrm{e}^{-\frac{|\xi|^2}{2}}\sum_{\kappa=0}^{\infty}\left(\frac{n!}{\kappa!}\right)^{\frac{1}{2}}(\xi)^{\kappa-n}L_n^{(\kappa-n)}\left(|\xi|^2\right)|\kappa\rangle. \tag{15}$$

Here, the generalized Laguerre polynomials are defined as

$$L_n^{(\eta)}(x) = \sum_{i=0}^{n}\binom{n+\eta}{n-i}\frac{(-1)^i}{i!}x^i, \tag{16}$$

where η is an integer. Using equations (12) and (15), we can calculate the general forms of the expectation values of the conjugate momentum $\hat{P}_x$ and position operator $\hat{X}$ under the final pointer states $|\phi_{f_1}\rangle$, which are given by

$$\langle X\rangle_{f_1}^{\rm HG} = |\lambda|^2 g\,\Re\langle A\rangle_w \tag{17}$$

and

$$2g\left\langle P_x\right\rangle_{f_1}^{\rm HG} = |\lambda|^2 s^2\,\Im\langle A\rangle_w\,\mathrm{e}^{-\frac{s^2}{4}} \times\sum_{\kappa=0}^{\infty}\frac{n!\left(\frac{-s^2}{4}\right)^{\kappa-n}}{\kappa!}L_n^{(\kappa-n)}\left(\frac{s^2}{4}\right)L_n^{(\kappa-n+1)}\left(\frac{s^2}{4}\right), \tag{18}$$

respectively. Equations (17), (18) are the general forms of expectation values for the system operator $\hat{A}$ satisfying $\hat{A}^2 = \hat{I}$, and they are valid for an arbitrary value of the measurement-strength parameter s.

To investigate the practical advantages of the higher-order Gaussian modes, we check the SNR in two cases. Here, we consider the two-dimensional quantum (qubit) state and assume that the operator $\hat{A}$ to be observed is the x-component of the spin of a spin-1/2 particle through the von Neumann interaction (2)

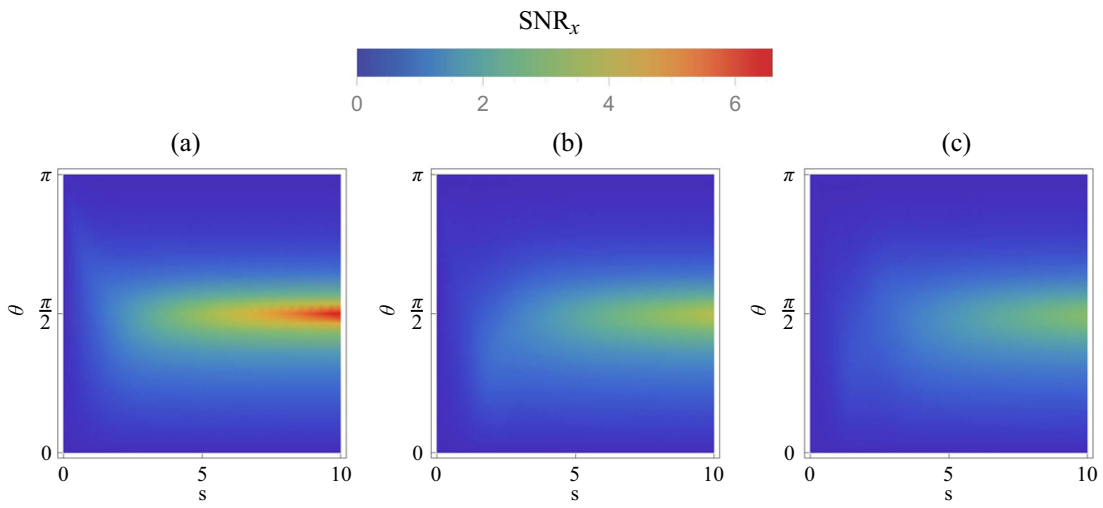

Figure 1. SNR in the x-direction for HG-mode pointer states with the operator $\hat{A}$ satisfying the property $\hat{A}^2 = \hat{I}$ plotted with respect to the measurement-strength parameter s and pre-selection angle θ for the mode (a) $n = 0$, (b) $n = 1$, and (c) $n = 2$. We use $\phi = 0$ in equation (22) in all figures.

$$\hat{A} = \hat{\sigma}_x = \left| \uparrow_z \right\rangle \left\langle \downarrow_z \right| + \left| \downarrow_z \right\rangle \left\langle \uparrow_z \right|. \tag{19}$$

Here, $|\uparrow_z\rangle$ and $|\downarrow_z\rangle$ are eigenstates of $\hat{\sigma}_z$ with corresponding eigenvalues of 1 and -1, respectively. We select the pre- and post-selected states as

$$\left|\psi_i\right\rangle = \cos\left(\frac{\theta}{2}\right)\left|\uparrow_z\right\rangle + e^{i\phi}\sin\left(\frac{\theta}{2}\right)\left|\downarrow_z\right\rangle \tag{20}$$

and

$$\left|\psi_f\right\rangle = \left|\uparrow_z\right\rangle, \tag{21}$$

respectively. Thus, we can obtain the weak value by substituting these states into equation (3):

$$\langle A\rangle_w = e^{i\phi}\tan\frac{\theta}{2}, \tag{22}$$

where $\theta \in [0, \pi]$ and $\phi \in [0, 2\pi)$. Here, the probability of post-selection is $P_s = \cos^2(\theta/2)$. Throughout the present paper, these pre- and post-selected states are used in the analysis of SNRs.

In figure 1, the behavior of the SNR is shown as a function of the measurement-strength parameter s and pre-selection angle θ. When $\phi = 0$, the weak value becomes $\tan\frac{\theta}{2}$. We can see that the SNR decreases as n increases (higher-order modes). A ridge exists around $\theta = \pi/2$, which is a result of strong measurement; when $\theta = \pi/2$, the pre-selection state is the eigenstate of the operator $\hat{\sigma}_x$ with the corresponding eigenvalue $+1$. In figure 1, we can also identify a bridge between the weak measurement regime ($s \ll 1$) and strong measurement regime ($s \gg 1$). As the SNR is proportional to the root of the measurement time, we consider $N = 1$ throughout this paper. These results show that the fundamental Gaussian pointer state is better than the other HG modes on the improvement of the SNR.

We also check the SNR with some specific weak values, and the numerical results are given in figure 2. As shown in figures 1 and 2, the higher-order HG modes have no practical advantages in improving the SNR. We also note that the imaginary part of the weak value has no role in improving the SNR in the x-direction. These results are in general supported by [22, 78].

3.2. $\hat{A}^2 = \hat{A}$ case

By following the process used for the $\hat{A}^2 = \hat{I}$ case, we can obtain the normalized final pointer states after the unitary evolution given in equation (5). The post-selection to $|\psi_f\rangle$ is given as follows:

$$\left|\phi_{f_2}\right\rangle = \gamma\left[1 - \langle A\rangle_w + \langle A\rangle_w D\left(\frac{s}{2}\right)\right]\left|\phi_i\right\rangle, \tag{23}$$

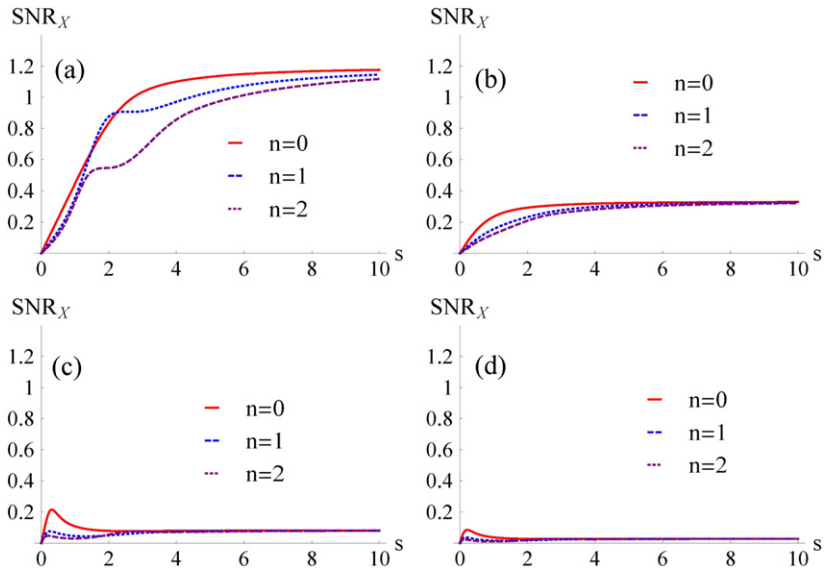

Figure 2. SNR in the x-direction for HG-mode pointer states with the operator $\hat{A}$ satisfying the property $\hat{A}^2 = \hat{I}$ plotted with respect to the measurement-strength parameter s for some specific weak values: (a) $\langle A\rangle_w = 0.5$, (b) $\langle A\rangle_w = 0.5+\mathrm{i}$, (c) $\langle A\rangle_w = 5$, and (d) $\langle A\rangle_w = 5+5\mathrm{i}$ [9].

where γ is the normalization coefficient given by

$$\gamma = \left[1 + 2\left(\Re\langle A\rangle_w - \left|\langle A\rangle_w\right|^2\right)\left(\mathrm{e}^{-\frac{s^2}{8}} L_n\left(\frac{s^2}{4}\right) - 1\right)\right]^{-\frac{1}{2}}. \tag{24}$$

Thus, by using equations (15) and (23), we can calculate the general forms of expectation values of the conjugate momentum $\hat{P}_x$ and position operator $\hat{X}$ under the final pointer sates $|\phi_{f_2}\rangle$; the obtained results are given by

$$\langle X\rangle_{f_2}^{\mathrm{HG}} = |\gamma|^2 g\left(\Re\langle A\rangle_w - \left|\langle A\rangle_w\right|^2\right)\mathrm{e}^{-\frac{s^2}{8}} L_n\left(\frac{s^2}{4}\right) + |\gamma|^2 g\left|\langle A\rangle_w\right|^2 \tag{25}$$

and

$$2g\left\langle P_x\right\rangle_{f_2}^{\mathrm{HG}} = |\gamma|^2 s^2 \Im\langle A\rangle_w \mathrm{e}^{-\frac{s^2}{8}}\left(L_n^{(1)}\left(\frac{s^2}{4}\right) + L_{n-1}^{(1)}\left(\frac{s^2}{4}\right)\right), \tag{26}$$

respectively. In these calculations, we use the following properties of the displaced Fock states [79]:

$${}_{\mathrm{HG}}\langle n+d|\, D(\xi)\,|n\rangle_{\mathrm{HG}} = \sqrt{\frac{n!}{(n+d)!}}\,\mathrm{e}^{-\frac{|\xi|^2}{2}}\xi^d L_n^{(d)}\left(|\xi|^2\right), \tag{27}$$

$${}_{\mathrm{HG}}\langle n|\, D(\xi)\,|n+d\rangle_{\mathrm{HG}} = \sqrt{\frac{n!}{(n+d)!}}\,\mathrm{e}^{-\frac{|\xi|^2}{2}}\left(-\xi^\star\right)^d L_n^{(d)}\left(|\xi|^2\right), \tag{28}$$

$${}_{\mathrm{HG}}\langle n|\, D(\xi)\,|n\rangle_{\mathrm{HG}} = \mathrm{e}^{-\frac{|\xi|^2}{2}} L_n\left(|\xi|^2\right). \tag{29}$$

We know that the operator $\hat{A}$ satisfying the property $\hat{A}^2 = \hat{A}$ can be a projection operator $\hat{A} = |C\rangle\langle C|$ that can also be taken as $\hat{A} = (\hat{I} \pm \hat{B})/2$ with $\hat{B}^2 = \hat{I}$. This type of operator has numerous applications in the weak measurement theory, such as in the three-box paradox problem [30] and quantum tomography [40, 41]. In the present paper, we consider $\hat{A} = (\hat{I} + \hat{\sigma_x})/2$ and choose the pre- and post-selected states as given in equations (20) and (21), respectively. The numerical results are shown in figure 3. As indicated in figure 3, the higher-order HG modes have no practical advantages in improving the SNR for the operator $\hat{A}$ satisfying the property $\hat{A}^2 = \hat{A}$, and the imaginary part of the weak values has no role in increasing the SNR, as mentioned above.

[9] In equation (22), $\langle A\rangle_w = 0.5$ is about $\phi = 0$, $\theta = 0.927$, $\langle A\rangle_w = \mathrm{i}$ is $\phi = \pi/2$, $\theta = \pi/2$, $\langle A\rangle_w = 0.5 + \mathrm{i}$ is about $\phi = 1.11$, $\theta = 1.68$, $\langle A\rangle_w = 1 + \mathrm{i}$ is about $\phi = 0.785$, $\theta = 1.91$, $\langle A\rangle_w = 5$ is about $\phi = 0$, $\theta = 2.74$, $\langle A\rangle_w = 5\mathrm{i}$ is about $\phi = \pi/2$, $\theta = 2.74$, and $\langle A\rangle_w = 5 + 5\mathrm{i}$ is about $\phi = 0.785$, $\theta = 2.86$.

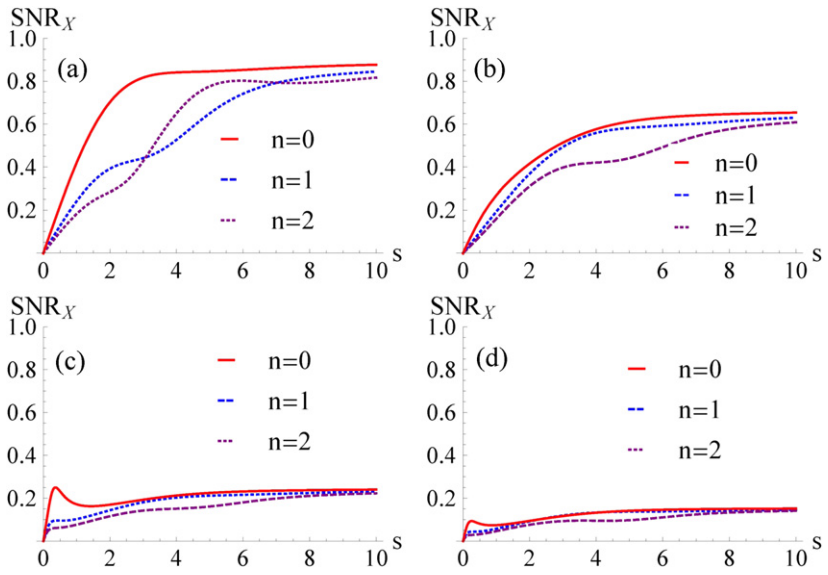

Figure 3. SNR in the x-direction for HG-mode pointer states with the operator $\hat{A}$ satisfying the property $\hat{A}^2 = \hat{A}$ plotted with respect to the measurement-strength parameter s for some specific weak values: (a) $\langle A\rangle_w = 0.5$, (b) $\langle A\rangle_w = 0.5 + \mathrm{i}$, (c) $\langle A\rangle_w = 5$, and (d) $\langle A\rangle_w = 5 + 5\mathrm{i}$ (see footnote 9).

4. Post-selected von Neumann measurements with LG-mode pointer states

The general LG modes can be defined as [70, 71]

$$|\mu, \nu\rangle_{\mathrm{LG}} = \left(\frac{1}{2}\right)^{\frac{\alpha+\beta}{2}} \frac{1}{\sqrt{\alpha!\beta!}} \left(\hat{a}_x^\dagger + \mathrm{i}\hat{a}_y^\dagger\right)^\alpha \left(\hat{a}_x^\dagger - \mathrm{i}\hat{a}_y^\dagger\right)^\beta |0,0\rangle_{\mathrm{HG}}, \tag{30}$$

where ν and μ are integers. Here, the indices $\alpha = (\mu + \nu)/2$ and $\beta = (\mu - \nu)/2$ are related to the usual radial and azimuthal indices (p and l, respectively) by the relations $p = \min(\alpha, \beta)$ and $l = |\alpha - \beta|$. We let $|0,0\rangle_{\mathrm{HG}}$ denote the HG-mode fundamental Gaussian state. If we use the binomial formula for equation (30), we can find a more explicit form of LG-mode pointer states as a sum of HG modes:

$$|\mu, \nu\rangle_{\mathrm{LG}} = \sum_{j=0}^{\alpha}\sum_{k=0}^{\beta} C_{\alpha,j;\beta,k}\, |\alpha + \beta - k - j,\, k + j\rangle_{\mathrm{HG}}. \tag{31}$$

Here, we note that $C_{\alpha,j;\beta,k}$ is given by

$$C_{\alpha,j;\beta,k} = \left(\frac{1}{\sqrt{2}}\right)^{\alpha+\beta} \frac{(-1)^k (i)^{k+j}}{\sqrt{\alpha!\beta!}} \times \sqrt{(\alpha + \beta - k - j)!\,(k + j)!} \binom{\alpha}{j}\binom{\beta}{k}. \tag{32}$$

In the present paper, we take the initial state of the LG-mode pointer as $|\varphi_i\rangle = |\mu, \nu\rangle_{\mathrm{LG}}$.

The LG modes are a complete set of solutions to the paraxial wave equation in cylindrical coordinates characterized by radial and azimuthal indexes p and l [65]. Physically, the LG modes have been created using various experimental setups such as SLMs [80] and reflection from a conical mirror [81]. Furthermore, the LG modes have a zero-intensity point at the center called the optical vortex. The relationship between the optical vortex and the weak value has been investigated from different perspectives [13, 69, 82–85]. Thus, a general treatment of the post-selected von Neumann measurements with LG-mode pointer states will provide an efficient method for further exploration of weak-value applications in higher-order optical beams and optical vortices. Next, we present an explicit treatment of post-selected von Neumann measurements with LG-mode pointer states for the system operator $\hat{A}$ that satisfies the properties $\hat{A}^2 = \hat{I}$ and $\hat{A}^2 = \hat{A}$.

4.1. $\hat{A}^2 = \hat{I}$ case

By using the same process as that used in the HG-mode cases, after the unitary evolution given in equation (4) and the post-selection of the system to $|\psi_f\rangle$, we can obtain the normalized final-pointer states as

$$\left|\varphi_{f_1}\right\rangle = \frac{\lambda'}{2}\left[D\left(\frac{s}{2}\right) + D\left(-\frac{s}{2}\right) + \langle A\rangle_w\left\{D\left(\frac{s}{2}\right) - D\left(-\frac{s}{2}\right)\right\}\right]|\mu,\,\nu\rangle_{\mathrm{LG}}, \tag{33}$$

where the normalization coefficient is given by

$$\lambda' = \left[1 + \frac{1}{2}\left(1 - \left|\langle A\rangle_w\right|^2\right) \times \left(\mathrm{e}^{-\frac{s^2}{2}}\sum_{j,j'=0}^{\alpha}\sum_{k,k'=0}^{\beta} C_{\alpha,j;\beta,k}C^{\star}_{\alpha,j';\beta,k'}\delta_{k'+j',k+j}L_{\alpha+\beta-k-j}\left(s^2\right) - 1\right)\right]^{-\frac{1}{2}}. \tag{34}$$

By using equation (33) and the displaced Fock states, i.e. equation (15), we can obtain the expectation value of the position operator $\hat{X}$ under the final pointer states $|\varphi_{f_1}\rangle$ as

$$\langle X\rangle^{\mathrm{LG}}_{f_1} = g\left|\lambda'\right|^2\Re\langle A\rangle_w. \tag{35}$$

Similarly, the expectation value of the momentum operator $\hat{P}_x$ under the final pointer states $|\varphi_{f_1}\rangle$ is given by

$$\begin{aligned} 2g\left\langle P_x\right\rangle^{\mathrm{LG}}_{f_1} = {} & \left|\lambda'\right|^2 s^2\Im\langle A\rangle_w\mathrm{e}^{-\frac{s^2}{4}}\sum_{j,j'=0}^{\alpha}\sum_{k,k'=0}^{\beta} C_{\alpha,j;\beta,k}C^{\star}_{\alpha,j';\beta,k'}\delta_{k'+j',k+j} \\ & \times\sum_{l=0}^{\infty}\frac{(\alpha+\beta-k-j)!\left(-\frac{s^2}{4}\right)^{l-(\alpha+\beta-k-j)}}{l!} \\ & \times L^{(l-(\alpha+\beta-k-j))}_{\alpha+\beta-k-j}\left(\frac{s^2}{4}\right)L^{(l+1-(\alpha+\beta-k-j))}_{\alpha+\beta-k-j}\left(\frac{s^2}{4}\right). \end{aligned} \tag{36}$$

From the definitions of the HG and LG modes in the Fock state representation, i.e. equations (11) and (31), respectively, we can see that the LG modes are not factorable into functions depending only on x and y, in contrast to the HG modes. This feature of the LG modes causes the coupling of the system observable $\hat{A}$ with the x- and y-dimension of the pointer. Thus, the pointer also shifts values in the y-direction. The pointer value is given by

$$\begin{aligned} \langle Y\rangle^{\mathrm{LG}}_{f_1} = {} & g\left|\lambda'\right|^2\Im\langle A\rangle_w\mathrm{e}^{-\frac{s^2}{2}}\sum_{j,j'=0}^{\alpha}\sum_{k,k'=0}^{\beta}\Re\left\{\mathrm{i}C_{\alpha,j;\beta,k}C^{\star}_{\alpha,j';\beta,k'}\right\} \\ & \times\delta_{k'+j',k+j-1}\sqrt{\frac{k+j}{(\alpha+\beta-k-j+1)}}L^{(1)}_{\alpha+\beta-k-j}\left(s^2\right) \\ & - g\left|\lambda'\right|^2\Im\langle A\rangle_w\mathrm{e}^{-\frac{s^2}{2}}\sum_{j,j'=0}^{\alpha}\sum_{k,k'=0}^{\beta}\Re\left\{\mathrm{i}C_{\alpha,j;\beta,k}C^{\star}_{\alpha,j';\beta,k'}\right\} \\ & \times\delta_{k'+j',k+j+1}\sqrt{\frac{k+j+1}{(\alpha+\beta-k-j)}}L^{(1)}_{\alpha+\beta-k-j-1}\left(s^2\right). \end{aligned} \tag{37}$$

These expectation values are the general forms of the desired values in post-selected von Neumann measurements with LG pointer states for the system operator $\hat{A}$ satisfying the property $\hat{A}^2 = \hat{I}$.

For the weak value (22) with $\phi = 0$ fixed, the SNR is determined to be a function of the coupling parameter s and the pre-selection angle θ for lower radial and azimuthal indices p and l, respectively, as shown in figure 4. In the figure, we show plots only for $p = 0,\ 1,\ 2$ and the corresponding $l = 0,\ 1,\ 2$ cases. Furthermore, by selecting specific weak values, we plot the SNR as a function of the measurement-strength parameter s, as shown in figure 5. From figures 4 and 5, we can see that the higher-order LG modes have no advantages in improving the SNR over the case of the fundamental Gaussian mode (corresponding to the $p = 0, l = 0$ case). From figure 5, we can also see that the imaginary part of the weak value has no role in improving the SNR in the x-direction.

The SNR for the y-direction shift is shown in figures 6 and 7. In figure 6, the SNRs for the lower-order cases of LG modes are shown, while in figure 7, the SNR in the y-direction is plotted as a function of the measurement-strength parameter s for some specific weak values with the radial index fixed at $p = 0$ and azimuthal index l increasing. We can observe that the SNR in the y-direction is related to the azimuthal indices l, while the SNR decreases as the radial indices p are increased (see figure 6). Thus, when $l = 0$, there is no information about the y-direction. We should emphasize that while the maximum of the y-direction shift is very small compared to that of the x-direction shift, in the weak measurement regime, the y-direction shift is sufficiently large compared to the x-direction shift. In figure 7, we can also observe that the real part of the weak value has no role in improving

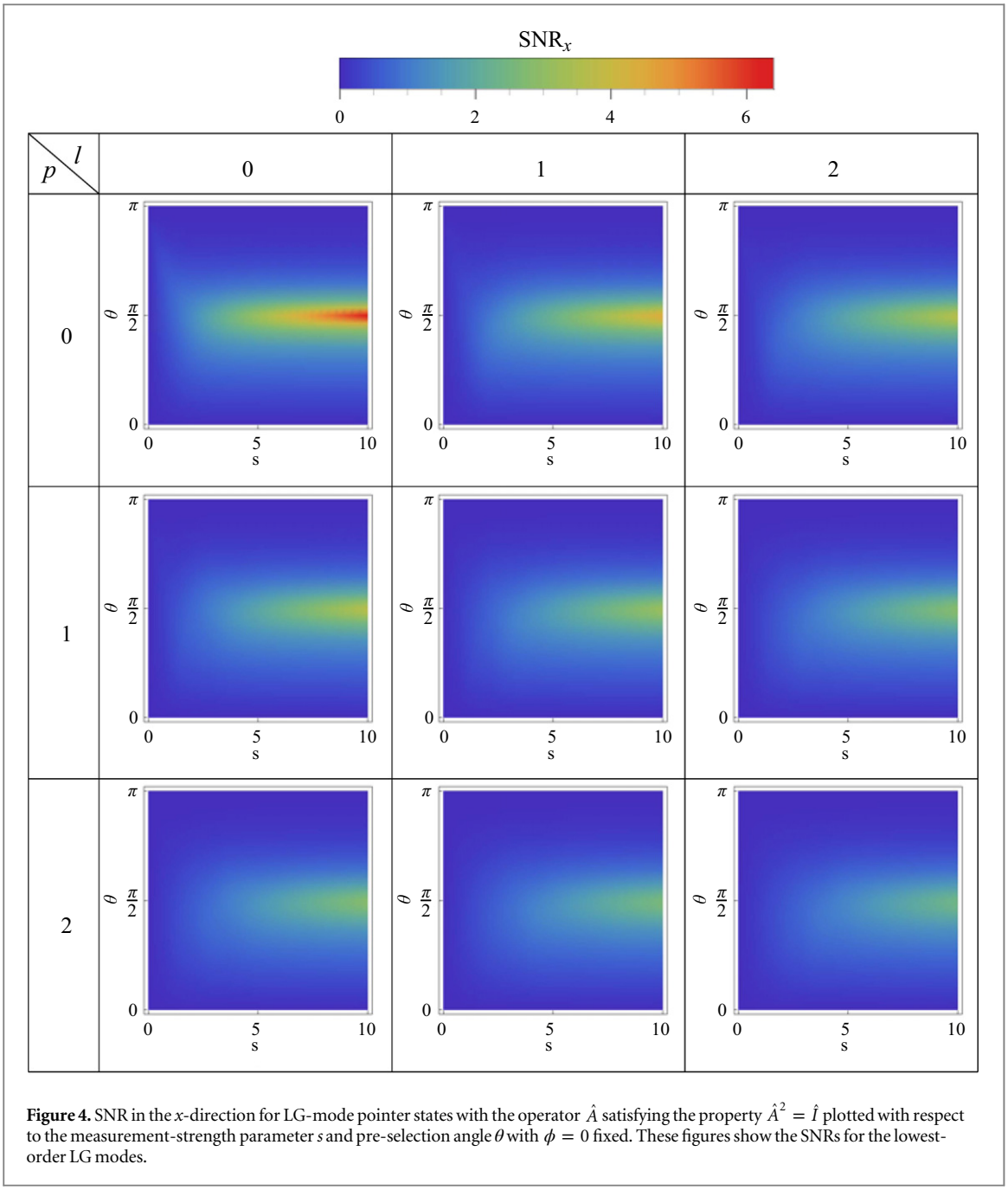

Figure 4. SNR in the x-direction for LG-mode pointer states with the operator $\hat{A}$ satisfying the property $\hat{A}^2 = \hat{I}$ plotted with respect to the measurement-strength parameter s and pre-selection angle θ with $\phi = 0$ fixed. These figures show the SNRs for the lowest-order LG modes.

the SNR in the y-direction. Because there is no direct interaction between the pointer and the measured system along the y-direction, the strong measurement regime ($s \gg 1$) includes only the x-direction shift. In the weak measurement regime, however, the pointer state can be shifted along not only the x-direction but also the y-direction because the unfactorability of the LG modes induces y-direction interference for x-direction interaction. On the improvement of the SNR in the y-direction, it seems to be converged to the specific value on increasing the azimuthal indices l.

4.2. $\hat{A}^2 = \hat{A}$ case

Using a process similar to that in the previous section, we can determine the normalized final state of the LG-mode pointer states as follows:

$$\left|\varphi_{f_2}\right\rangle = \gamma'\left[1 - \langle A\rangle_w + \langle A\rangle_w D\left(\frac{g}{2\sigma}\right)\right]|\mu, \nu\rangle_{\mathrm{LG}}, \tag{38}$$

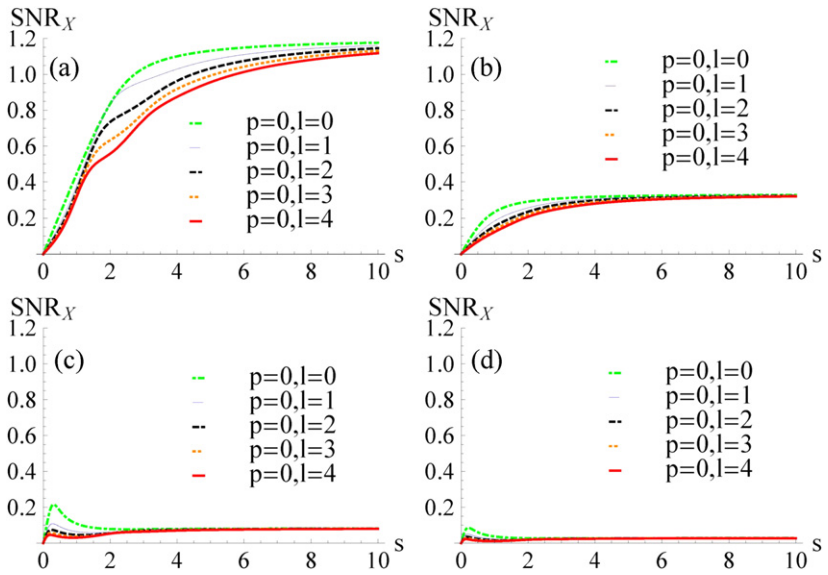

Figure 5. SNR in the x-direction for LG-mode pointer states with the operator $\hat{A}$ satisfying the property $\hat{A}^2 = \hat{I}$ plotted with respect to the measurement-strength parameter s for some specific weak values: (a) $\langle A\rangle_w = 0.5$, (b) $\langle A\rangle_w = 0.5 + \mathrm{i}$, (c) $\langle A\rangle_w = 5$, and (d) $\langle A\rangle_w = 5 + 5\mathrm{i}$ (see footnote 9).

for the normalization coefficient

$$\gamma' = \left[1 + 2\left(\Re\langle A\rangle_w - \left|\langle A\rangle_w\right|^2\right) \times \left(\mathrm{e}^{-\frac{s^2}{8}} \sum_{j,j'=0}^{\alpha} \sum_{k,k'=0}^{\beta} C_{\alpha,j;\beta,k} C^{\star}_{\alpha,j';\beta,k'} \delta_{k'+j',k+j} L_{\alpha+\beta-k-j}\left(\frac{s^2}{4}\right) - 1\right)\right]^{-\frac{1}{2}}. \tag{39}$$

The expectation values of the position operators $\hat{X}$, $\hat{Y}$, and the momentum operator $\hat{P}_x$ under the final state $|\varphi_{f_2}\rangle$ are given by

$$\begin{aligned}\langle X\rangle^{\mathrm{LG}}_{f_2} = {} & \left|\gamma'\right|^2 g\left(\Re\langle A\rangle_w - \left|\langle A\rangle_w\right|^2\right)\mathrm{e}^{-\frac{s^2}{8}} \\ & \times \sum_{j,j'=0}^{\alpha} \sum_{k,k'=0}^{\beta} C_{\alpha,j;\beta,k} C^{\star}_{\alpha,j';\beta,k'} \delta_{k'+j',k+j} L_{\alpha+\beta-k-j}\left(\frac{s^2}{4}\right) \\ & + g\left|\gamma'\right|^2 \left|\langle A\rangle_w\right|^2,\end{aligned} \tag{40}$$

$$\begin{aligned}\langle Y\rangle^{\mathrm{LG}}_{f_2} = {} & -g\left|\gamma'\right|^2 \Im\langle A\rangle_w \mathrm{e}^{-\frac{s^2}{8}} \sum_{j,j'=0}^{\alpha} \sum_{k,k'=0}^{\beta} \Re\left\{\mathrm{i} C_{\alpha,j;\beta,k} C^{\star}_{\alpha,j';\beta,k'}\right\} \\ & \times \delta_{k'+j',k+j+1} \sqrt{\frac{k+j+1}{\alpha+\beta-k-j}} L^{(1)}_{\alpha+\beta-k-j-1}\left(\frac{s^2}{4}\right) \\ & + g\left|\gamma'\right|^2 \Im\langle A\rangle_w \mathrm{e}^{-\frac{s^2}{8}} \sum_{j,j'=0}^{\alpha} \sum_{k,k'=0}^{\beta} \Re\left\{\mathrm{i} C_{\alpha,j;\beta,k} C^{\star}_{\alpha,j';\beta,k'}\right\} \\ & \times \delta_{k'+j',k+j-1} \sqrt{\frac{k+j}{\alpha+\beta-k-j+1}} L^{(1)}_{\alpha+\beta-k-j}\left(\frac{s^2}{4}\right),\end{aligned} \tag{41}$$

and

$$\begin{aligned}2g\left\langle P_x\right\rangle^{\mathrm{LG}}_{f_2} = {} & \left|\gamma'\right|^2 s^2 \Im\langle A\rangle_w \mathrm{e}^{-\frac{s^2}{8}} \sum_{j,j'=0}^{\alpha} \sum_{k,k'=0}^{\beta} C_{\alpha,j;\beta,k} C^{\star}_{\alpha,j';\beta,k'} \\ & \times \delta_{k'+j',k+j}\left[L^{(1)}_{\alpha+\beta-k-j}\left(\frac{s^2}{4}\right) + L^{(1)}_{\alpha+\beta-k-j-1}\left(\frac{s^2}{4}\right)\right],\end{aligned} \tag{42}$$

respectively.

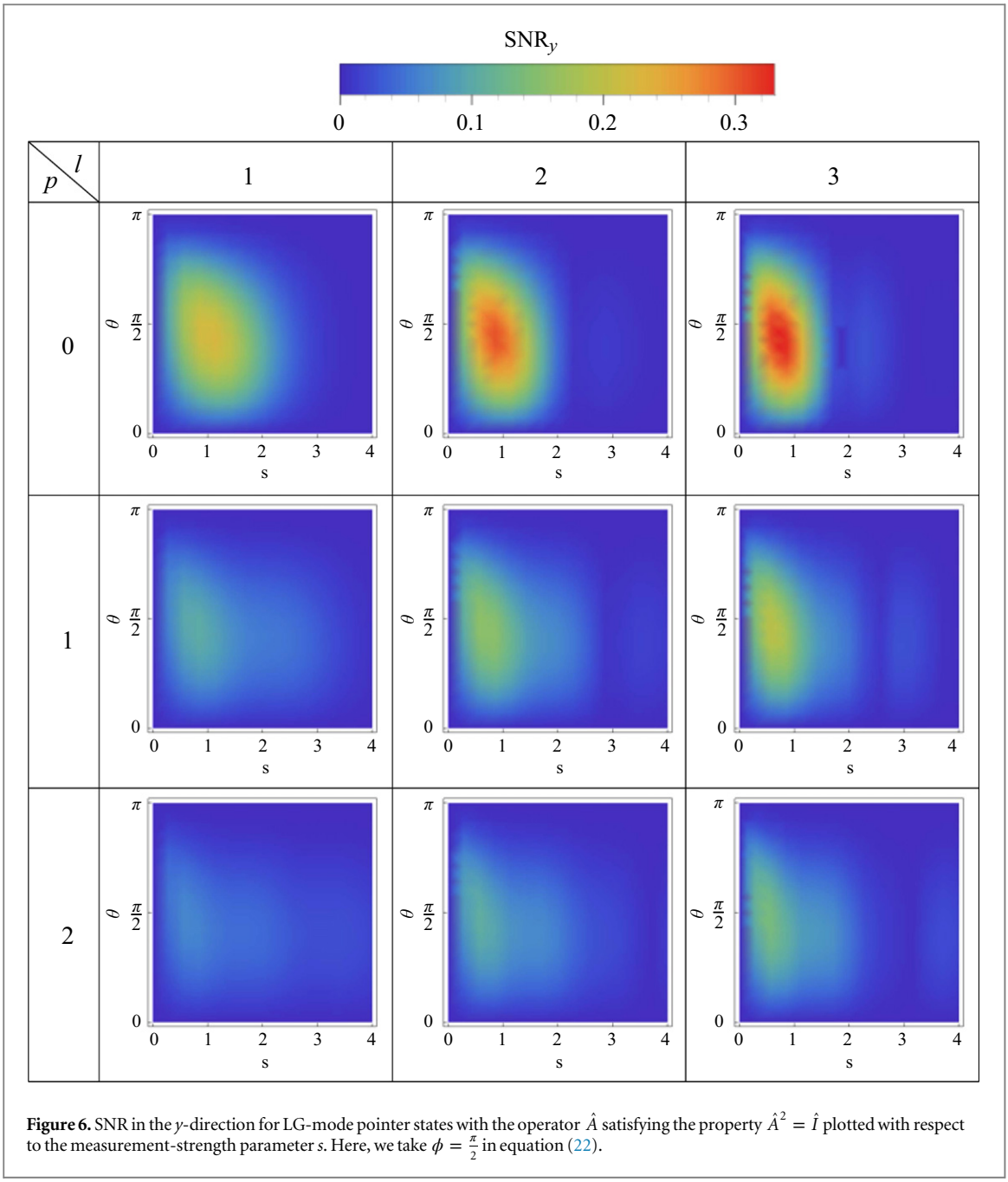

Figure 6. SNR in the y-direction for LG-mode pointer states with the operator $\hat{A}$ satisfying the property $\hat{A}^2 = \hat{I}$ plotted with respect to the measurement-strength parameter s. Here, we take $\phi = \frac{\pi}{2}$ in equation (22).

For LG-mode pointer states with the system operator $\hat{A}$ satisfying the property $\hat{A}^2 = \hat{A}$, we verify the SNR values in the x- and y-direction as functions of measurement-strength parameter s with some specific weak values, and the numerical results are given in figures 8 and 9, respectively. For the SNR in the x-direction, we reach the same conclusions as before: the higher-order LG modes and imaginary parts of the weak value have no advantages in improving the SNR in the x-direction (see figure 8).

In figure 9, we plot the SNR curves in the y-direction with the radial index fixed at $p = 0$ and azimuthal index l changing. From figure 9, we can observe that in the weak measurement regime ($s \ll 1$), the SNR in the y-direction is improved in comparison with the case $\hat{A}^2 = \hat{I}$ shown in figure 7. We numerically find that the maximum value of the SNR occurs for $\langle A \rangle_w = 0.5 + \mathrm{i}$, as shown in figure 9(e). The maximum condition of this SNR corresponds to the minimum condition for equation (39). Furthermore, from figure 9, we also can see that when the azimuthal index l increases, the SNR in the y-direction increases for a fixed radial index p. When the coupling between the system (x-direction) and the pointer devices is sufficiently strong, the SNR in the y-direction gradually vanishes. From figure 9, we can further deduce that the real part of the weak value has no role in improving the SNR in the y-direction. Note that these results investigate the importance of the imaginary part of the weak value such as [22, 78]. Also, there still is the open problem whether the unified information of the x -and y-directions is useful as the optical implementation of the parameter estimation.

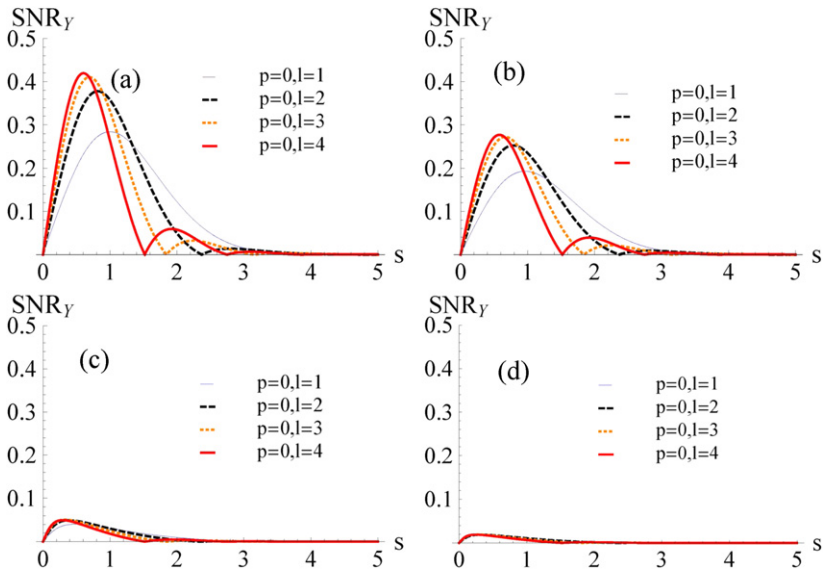

Figure 7. SNR in the y-direction for LG-mode pointer states with the operator $\hat{A}$ satisfying the property $\hat{A}^2 = \hat{I}$ for (a) $\langle A\rangle_w = \mathrm{i}$, (b) $\langle A\rangle_w = 0.5 + \mathrm{i}$, (c) $\langle A\rangle_w = 5\mathrm{i}$, and (d) $\langle A\rangle_w = 5 + 5\mathrm{i}$ (see footnote 9).

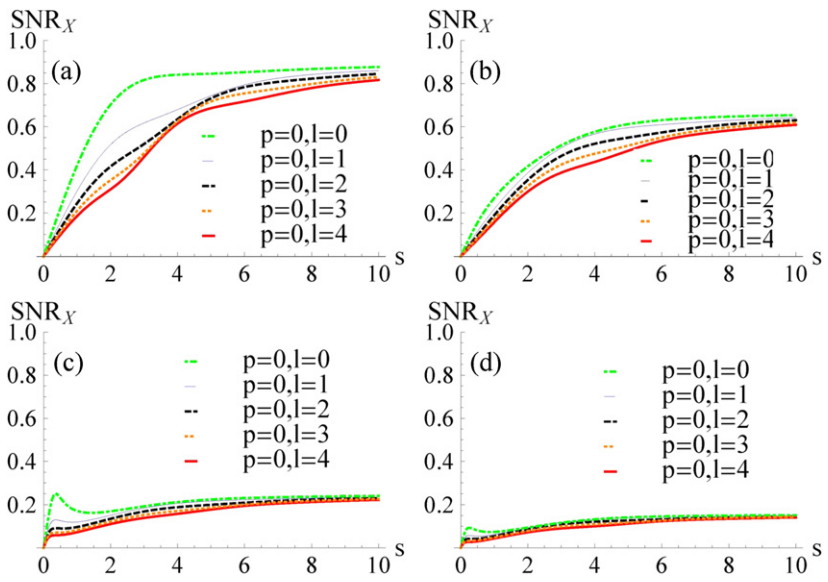

Figure 8. SNR in the x-direction for LG-mode pointer states with the operator $\hat{A}$ satisfying the property $\hat{A}^2 = \hat{A}$ plotted with respect to the measurement-strength parameter s for specific weak values: (a) $\langle A\rangle_w = 0.5$, (b) $\langle A\rangle_w = 0.5 + \mathrm{i}$, (c) $\langle A\rangle_w = 5$, and (d) $\langle A\rangle_w = 5 + 5\mathrm{i}$ (see footnote 9).

5. Some approximation cases

5.1. $\hat{A}^2 = \hat{I}$ case

If we take the fundamental Gaussian beam as the initial pointer state (this corresponds to taking $m = n = 0$ and $\alpha = \beta = 0$ in equations (11) and (30), respectively), the general expectation values for position operator $\hat{X}$, i.e. equations (17) and (35), and momentum operator $\hat{P}$, i.e. equations (18) and (36), are reduced to

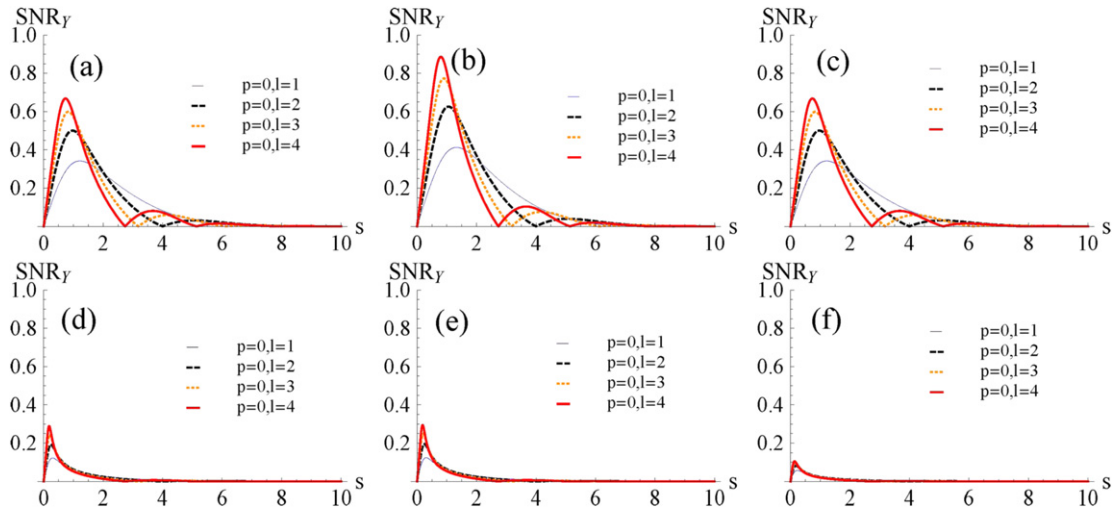

Figure 9. SNR in the y-direction for LG-mode pointer states with the operator $\hat{A}$ satisfying the property $\hat{A}^2 = \hat{A}$ plotted with respect to the measurement-strength parameter s for specific weak values: (a) $\langle A\rangle_w = \mathrm{i}$, (b) $\langle A\rangle_w = 0.5 + \mathrm{i}$, (c) $\langle A\rangle_w = 1 + \mathrm{i}$, (d) $\langle A\rangle_w = 5\mathrm{i}$, (e) $\langle A\rangle_w = 0.5 + 5\mathrm{i}$, and (f) $\langle A\rangle_w = 5 + 5\mathrm{i}$ (see footnote 9).

$$\langle X\rangle_{f_1,\mathrm{FG}} = \frac{g\Re\langle A\rangle_w}{\mathcal{Z}} \tag{43}$$

and

$$\left\langle P_x\right\rangle_{f_1,\mathrm{FG}} = \frac{g\Im\langle A\rangle_w}{2\sigma^2\mathcal{Z}}\mathrm{e}^{-\frac{s^2}{2}}, \tag{44}$$

respectively, where

$$\mathcal{Z} = 1 + \frac{1}{2}\left(1 - \left|\langle A\rangle_w\right|^2\right)\left(\mathrm{e}^{-\frac{s^2}{2}} - 1\right). \tag{45}$$

These results were also presented in [59].

Furthermore, under the weak measurement regime ($s \ll 1$), if we only consider evolution up to the first order, our general expectation values reproduce the results given in [70]. In this case, the HG and LG pointer states are shifted along x-direction with the same value, i.e.

$$\langle X\rangle_{f_1,\mathrm{first}} = g\Re\langle A\rangle_w. \tag{46}$$

The expectation value in the y-direction, i.e. equation (37), is reduced to

$$\langle Y\rangle^{\mathrm{LG}}_{f_1,\mathrm{first}} = -lg\Im\langle A\rangle_w. \tag{47}$$

The expectation value of the momentum operator for the HG-mode pointer states, i.e. equation (18), is reduced to

$$\left\langle P_x\right\rangle^{\mathrm{HG}}_{f_1,\mathrm{first}} = \frac{g\Im\langle A\rangle_w}{2\sigma^2}(2n+1), \tag{48}$$

while that for the LG-mode pointer states, i.e. equation (36), is reduced to

$$\left\langle P_x\right\rangle^{\mathrm{LG}}_{f_1,\mathrm{first}} = \frac{g\Im\langle A\rangle_w}{2\sigma^2}(2p+|l|+1). \tag{49}$$

The validity conditions for equations (46)–(49) are

$$\frac{g\sqrt{2n+1}}{2\sigma}\max\left(1, \left|\langle A\rangle_w\right|\right) \ll 1, \tag{50}$$

for the HG-mode pointer states, and

$$\frac{g\sqrt{2p+|l|+1}}{2\sigma}\max\left(1, \left|\langle A\rangle_w\right|\right) \ll 1, \tag{51}$$

for the LG-mode pointer states.

The SNRs are directly related to measurement-strength parameter s. Thus, in the strong measurement regime, if we take the limit $s \to \infty$, we notice that SNR_X becomes a function of the weak value

$$\left(\mathrm{SNR}_X\right)_{s\to\infty} = \frac{2\sqrt{P_s}\left|\Re\langle A\rangle_w\right|}{\sqrt{1+2\left|\langle A\rangle_w\right|^2+\left|\langle A\rangle_w\right|^4-4\Re^2\langle A\rangle_w}}. \tag{52}$$

We can observe this limiting trend from figures 2 and 5.

5.2. $\hat{A}^2 = \hat{A}$ case

If we take the fundamental Gaussian beam as the initial pointer states, the general expectation values for the position operator $\hat{X}$, i.e. equations (25) and (40), and momentum operator $\hat{P}_x$, i.e. equations (26) and (42), are reduced to

$$\langle X\rangle_{f_2,\mathrm{FG}} = g\frac{\left|\langle A\rangle_w\right|^2+\left(\Re\langle A\rangle_w-\left|\langle A\rangle_w\right|^2\right)\mathrm{e}^{-\frac{s^2}{8}}}{\mathcal{N}}, \tag{53}$$

and

$$\left\langle P_x\right\rangle_{f_2,\mathrm{FG}} = \frac{g\Im\langle A\rangle_w}{2\sigma^2\mathcal{N}}\mathrm{e}^{-\frac{s^2}{8}}, \tag{54}$$

respectively, where

$$\mathcal{N} = 1+2\left(\Re\langle A\rangle_w-\left|\langle A\rangle_w\right|^2\right)\left(\mathrm{e}^{-\frac{s^2}{8}}-1\right). \tag{55}$$

Furthermore, under the weak measurement regime ($s \ll 1$), if we only consider evolution up to the first order, our general expectation values are reduced to the following form:

$$\langle X\rangle_{f_2,\mathrm{first}} = g\Re\langle A\rangle_w. \tag{56}$$

In the case of the position operator $\hat{X}$, the HG mode and LG mode have the same value. The expectation value in the y-direction, equation (41), is reduced to

$$\langle Y\rangle^{\mathrm{LG}}_{f_2,\mathrm{first}} = -lg\Im\langle A\rangle_w. \tag{57}$$

For the momentum operator $\hat{P}_x$, the expectation values for the HG-mode pointer states, equation (26), and for the LG-mode pointer states, equation (42), are reduced to

$$\left\langle P_x\right\rangle^{\mathrm{HG}}_{f_2,\mathrm{first}} = \frac{g\Im\langle A\rangle_w}{2\sigma^2}(2n+1) \tag{58}$$

and

$$\left\langle P_x\right\rangle^{\mathrm{LG}}_{f_2,\mathrm{first}} = \frac{g\Im\langle A\rangle_w}{2\sigma^2}(2p+|l|+1), \tag{59}$$

respectively. The validity conditions for equations (56)–(59) are

$$\frac{g\sqrt{2n+1}}{2\sigma}\max\left(1,\left|\langle A\rangle_w\right|,\sqrt{\left|\Re\langle A\rangle_w\right|}\right)\ll 1, \tag{60}$$

for the HG-mode pointer states and

$$\frac{g\sqrt{2p+|l|+1}}{2\sigma}\max\left(1,\left|\langle A\rangle_w\right|,\sqrt{\left|\Re\langle A\rangle_w\right|}\right)\ll 1, \tag{61}$$

for the LG-mode pointer states.

For the SNR in the strong-measurement regime ($s \gg 1$), if we consider the limiting case of $s \to \infty$, we note that SNR_X becomes a function of the weak value

$$\left(\mathrm{SNR}_X\right)_{s\to\infty} = \frac{\sqrt{P_s}\left|\langle A\rangle_w\right|}{\sqrt{1+\left|\langle A\rangle_w\right|^2-2\Re\langle A\rangle_w}}. \tag{62}$$

We can observe this limiting trend from figures 3 and 8.

We emphasize here that the limiting values given in equations (52) and (62) are valid in the x-direction SNR for the HG- and LG-mode pointer states in corresponding lower-order modes. It is assumed that the probe wavefunction does not spread out during the interaction. Thus, for the case of the fundamental Gaussian pointer, the expectation values of the position operators (43), (53) and its conjugate momentum operators (44), (54) are the same as those in [86] under the weak-measurement condition.

6. Conclusion and remarks

In summary, we studied the post-selected von Neumann measurement with HG- and LG-mode pointer states for the system operator $\hat{A}$ satisfying $\hat{A}^2 = \hat{I}$ and $\hat{A}^2 = \hat{A}$. Our general expectation formulas are valid in not only the weak-measurement regime but also the strong-measurement regime. If we only consider evaluation up to the first order, our general results reproduce all results given in [70]. Moreover, if we let the initial pointer state be a fundamental Gaussian state, our general results reflect the full evaluation values given in [59].

To clarify the practical advantages of high-order Gaussian beams, we verified the SNR and found that the higher-order HG and LG modes have no advantages for improving the SNR over that for the case of the fundamental Gaussian mode. Moreover, we found that the imaginary part of the weak values has no role in improving the SNR in the x-direction in the cases of HG- and LG-mode pointer states. For the SNR in the y-direction in the LG-mode case, we also found that the SNR is related to the azimuthal index l and that the real part of the weak value has no role in improving the SNR in the y-direction. However, in the case of $\hat{A}^2 = \hat{I}$, the SNR in the y-direction has an upper bound even for increasing azimuthal indices l. In the case of $\hat{A}^2 = \hat{A}$, we observed an improvement in SNR in the y-direction in the weak-measurement regime because the SNR increases with increasing azimuthal index l. This fact may be helpful on the parameter estimation context as the optical implementation of the weak-value amplification. However, we found that the SNR in the y-direction gradually vanishes when the coupling strength between the system (x-direction) and pointer devices is increased. It is noted that our choice of the pre- and post-selection may be not optimal to maximize the SNR. The SNR in the y-direction also disappeared in the weak-measurement regime when the post-selected state is identical to the pre-selected one such that $\langle A\rangle_w = \langle \psi_i | A | \psi_i \rangle$.

These methods can provide a new technique for calculating the expectation values of the generation functions of the momentum and position operators. Thus, our results are useful for investigating applications of the weak-measurement theory in quantum dynamics and quantum correlations with higher-order optical beams. Also, these provide the role of the imaginary part of the weak value to lead to the complementarity relationship and the estimation problems in the Fourier domain for the LG higher order case.

We expect that our general treatment of the weak values will be helpful for understanding the connection between weak- and strong-measurement regimes and may be used to propose new experimental setups with higher-order Gaussian beams to investigate further the applications of weak measurement in optical systems such as the optical vortex. In this work, we only consider the pure higher-order HG and LG modes as initial pointer states and investigate the corresponding SNRs. However, the entanglement of the initial pointer states [87] and the non-classical initial pointer states [88] are useful for the weak-value amplification. Thus, our setup may provide another scheme for improving the SNR if we consider the initial state of the pointer as a coherent-superposition state of higher-order Gaussian beams.

Acknowledgments

Y T would like to thank Taximaiti Yusufu for useful suggestions and discussions. Y S thanks Shinji Yoshimura for discussions. This work was supported by a Grant for Basic Science Research Projects from The Sumitomo Foundation, a grant from Matsuo Foundation, IMS Joint Study Program, NINS youth collaborative projects, the Center for the Promotion of Integrated Sciences (CPIS) of Sokendai, ICRR Joint Research from The University of Tokyo, and JSPS KAKENHI Grant Numbers 24654133, 25790068, and 25287101. Y T acknowledges financial support from the IMS Internship project.

References

[1] von Neumann J 1955 *Mathematical Foundations of Quantum Mechanics* (Princeton, NJ: Princeton University Press) published in German, 1932
[2] Aharonov Y, Bergmann P G and Lebowitz J L 1964 *Phys. Rev.* **134** B1410
[3] Aharonov Y, Albert D Z and Vaidman L 1988 *Phys. Rev. Lett.* **60** 1351
[4] Kofman A G, Ashhab S and Nori F 2012 *Phys. Rep.* **520** 43
[5] Hosten O and Kwiat P 2008 *Science* **319** 787
[6] Dixon P B, Starling D J, Jordan A N and Howell J C 2009 *Phys. Rev. Lett.* **102** 173601
[7] Starling D J, Dixon P B, Jordan A N and Howell J C 2009 *Phys. Rev.* A **80** 041803(R)
[8] Hogan J M, Hammer J, Chiow S-W, Dickerson S, Johnson D M S, Kovachy T, Sugarbaker A and Kasevich M A 2011 *Opt. Lett.* **36** 1698
[9] Pfeifer M and Fischer P 2011 *Opt. Express* **19** 16508
[10] Zhou L, Turek Y, Sun C P and Nori F 2013 *Phys. Rev.* A **88** 053815
[11] Starling D J, Dixon P B, Jordan A N and Howell J C 2010 *Phys. Rev.* A **82** 063822
[12] Starling D J, Dixon P B, Williams N S, Jordan A N and Howell J C 2010 *Phys. Rev.* A **82** 011802(R)

[13] Magaña-Loaiza O S, Mirhosseini M, Rodenburg B and Boyd R W 2014 *Phys. Rev. Lett.* **112** 200401
[14] de Lima Bernardo B, Azevedo S and Rosas A 2014 *Phys. Lett.* A **378** 2029
[15] Viza G I, Martinez-Rincon J, Howland G A, Frosting H, Shromroni I, Dayan B and Howell J C 2013 *Opt. Lett.* **38** 2949
[16] Egan P and Stone J A 2012 *Opt. Lett.* **37** 4991
[17] Feizpour A, Xing X and Steinberg A M 2011 *Phys. Rev. Lett.* **107** 133603
[18] Tanaka S and Yamamoto N 2013 *Phys. Rev.* A **88** 042116
[19] Jordan A N, Martínez-Rincón J and Howell J C 2014 *Phys. Rev.* X **4** 011031
[20] Knee G C and Gauger E M 2014 *Phys. Rev.* X **4** 011032
[21] Lee J and Tsutsui I 2014 *Quantum Stud.: Math. Found.* **1** 65
[22] Knee G C, Combes J, Ferrie C and Gauger E M 2014 in preparation (arXiv:1410.6252)
[23] Combes J, Ferrie C, Jiang Z and Caves C M 2014 *Phys. Rev.* A **89** 052117
[24] Ferrie C and Combes J 2014 *Phys. Rev. Lett.* **113** 120404
[25] Matsuoka F, Tomita A and Shikano Y 2014 in preparation (arXiv:1410.8046)
[26] Aharonov Y, Botero A, Popescu S, Reznik B and Tollaksen J 2002 *Phys. Lett.* A **301** 130
[27] Lundeen J S and Steinberg A M 2009 *Phys. Rev. Lett.* **102** 020404
[28] Yokota K, Yamamoto T, Koashi M and Imoto N 2009 *New J. Phys.* **11** 033011
[29] Hosoya A and Shikano Y 2010 *J. Phys.* A **43** 385307
[30] Resch K J, Lundeen J S and Steinberg A M 2004 *Phys. Lett.* A **324** 125
[31] Aharonov Y and Rohrlich D 2005 *Quantum Paradoxes: Quantum Theory for the Perplexed* (Weinheim: Wiley)
[32] Aharonov Y and Vaidman L 2008 *Time in Quantum Mechanics* ed J G Muga, R Sala Mayato and I L Egusquiza vol 1 (Berlin: Springer) p 399
[33] Aharonov Y and Tollaksen J 2011 *Vision of Discovery: New Light on Physics, Cosmology, and Consciousness* ed R Y Chiao, M L Cohen, A J Legget, W D Phillips and C L Harper Jr (Cambridge: Cambridge University Press) p 105
[34] Shikano Y 2012 *Measurement in Quantum Mechanics* ed M R Pahlavani (Rijeka: InTech) p 75
[35] Kagami S, Shikano Y and Asahi K 2011 *Physica* E **43** 761
[36] Shikano Y and Tanaka S 2011 *Europhys. Lett.* **96** 40002
[37] Shikano Y, Kagami S, Tanaka S and Hosoya A 2011 *AIP Conf. Proc.* **1363** 177
[38] Hofmann H F and Ren C 2013 *Phys. Rev.* A **87** 062109
[39] Dressel J, Malik M, Miatto F M, Jordan A N and Boyd R W 2014 *Rev. Mod. Phys.* **86** 307
[40] Lundeen J S, Sutherland B, Patel A, Stewart C and Bamber C 2011 *Nature* **474** 188
[41] Lundeen J S and Bamber C 2012 *Phys. Rev. Lett.* **108** 070402
[42] Kocsis S, Braverman B, Ravets S, Stevens M J, Mirin R P, Shalm L K and Steinberg A M 2011 *Science* **332** 1170
[43] Braverman B and Simon C 2013 *Phys. Rev. Lett.* **110** 060406
[44] Salvail J Z, Agnew M, Johnson A S, Bolduc E, Leach J and Boyd R W 2013 *Nat. Photonics* **7** 316
[45] Malik M, Mirhosseini M, Lavery M P, Leach J, Padgett M J and Boyd R W 2014 *Nat. Commun.* **5** 3115
[46] Palacios-Laloy A, Mallet A F, Nguyen F, Bertet P, Vion D, Esteve D and Korotkov A N 2010 *Nat. Phys.* **6** 442
[47] Suzuki Y, Iinuma M and Hofmann H F 2012 *New J. Phys.* **14** 103022
[48] Dressel J, Broadbent C J, Howell J C and Jordan A N 2011 *Phys. Rev. Lett.* **106** 040402
[49] Goggin M E, Almeida M P, Barbieri M, Lanyon B P, O'Brien J L, White A G and Pryde G J 2011 *Proc. Natl Acad. Sci. USA* **108** 1256
[50] Emary C, Lambert N and Nori F 2014 *Rep. Prog. Phys.* **77** 016001
[51] Groen J P, Riste D, Tornberg L, Cramer J, de Groot P C, Picot T, Johansson G and DiCarlo L 2013 *Phys. Rev. Lett.* **111** 090506
[52] Rozema L A, Darabi A, Mahler D H, Hayat A, Soudagar Y and Steinberg A M 2012 *Phys. Rev. Lett.* **109** 100404
[53] Kaneda F, Baek S-Y, Ozawa M and Edamatsu K 2014 *Phys. Rev. Lett.* **112** 020402
[54] Aharonov Y and Botero A 2005 *Phys. Rev.* A **72** 052111
[55] di Lorenzo A and Egues J C 2008 *Phys. Rev.* A **77** 042108
[56] Wu S and Li Y 2011 *Phys. Rev.* A **83** 052106
[57] Zhu X, Zhang Y, Pang S, Qiao C, Liu Q and Wu S 2011 *Phys. Rev.* A **84** 052111
[58] Koike T and Tanaka S 2011 *Phys. Rev.* A **84** 062106
[59] Nakamura K, Nishizawa A and Fujimoto M K 2012 *Phys. Rev.* A **85** 012113
[60] Susa Y, Shikano Y and Hosoya A 2012 *Phys. Rev.* A **85** 052110
[61] Di Lorenzo A 2013 *Phys. Rev.* A **87** 046101
[62] Susa Y, Shikano Y and Hosoya A 2012 *Phys. Rev.* A **87** 046102
[63] Shikano Y 2014 *AIP Conf. Proc.* **1633** 84
[64] Kogelnik H and Li T 1966 *App. Opt.* **5** 1550
[65] Siegman A E 1986 *Lasers* (Mill Valley, CA: University Science Books)
[66] Puentes G, Hermosa N and Torres J P 2012 *Phys. Rev. Lett.* **109** 040401
[67] Dressel J and Jordan A N 2012 *Phys. Rev. Lett.* **109** 230402
[68] Kobayashi H, Puentes G and Shikano Y 2012 *Phys. Rev.* A **86** 053805
[69] Kobayashi H, Nonaka K and Shikano Y 2014 *Phys. Rev.* A **89** 053816
[70] de Lima Bernardo B, Azevedo S and Rosas A 2014 *Opt. Commun.* **331** 194
[71] Cohen-Tannoudji C, Diu B and Laloe F 2005 *Quantum Mechanics I* 2nd edn (New York: Wiley)
[72] Nienhuis G and Allen L 1993 *Phys. Rev.* A **48** 656
[73] Padgett M J, Arlt J, Simpson N B and Allen L 1996 *Am. J. Phys.* **64** 77
[74] Beijersbergen M W, Allen L, van der Veen H E L O and Woerdman J P 1993 *Opt. Commun.* **96** 123
[75] Maurer C, Jesacher A, Bernet S and Ritsch-Marte M 2011 *Laser Photonics Rev.* **5** 81
[76] Roy S M and Singh V 1982 *Phys. Rev.* D **25** 3413
[77] de Oliveira F A M, Kim M S, Knight P L and Buzek V 1990 *Phys. Rev.* A **41** 2645
[78] Dressel J and Jordan A 2012 *Phys. Rev.* A **85** 012107
[79] Ferraro A, Olivares S and Paris M G A 2005 *Gaussian States in Continuous Variable Quantum Information* (Bibliopolis: Napoli)
[80] Ando T, Ohatake Y, Matsumoto N, Inoue T and Fukuchi N 2009 *Opt. Lett.* **34** 34
[81] Kobayashi H, Nonaka K and Kitano M 2012 *Opt. Express* **20** 14064
[82] Dennis M R and Götte J B 2012 *New J. Phys.* **14** 073013

[83] Götte J B and Dennis M R 2012 *New J. Phys.* **14** 073016
[84] Dennis M R and Götte J B 2012 *Phys. Rev. Lett.* **109** 183903
[85] Götte J B and Dennis M R 2012 *Opt. Lett.* **38** 2295
[86] Jozsa R 2007 *Phys. Rev.* A **76** 044103
[87] Pang S, Dressel J and Brun T A 2014 *Phys. Rev. Lett.* **113** 030401
[88] Turek Y, Maimaiti W, Shikano Y, Sun C-P and Al-Amri M 2015 *Phys. Rev.* A **92** 022109